II International Conference on Particle-based Methods – Fundamentals and Applications
PARTICLES 2011
E. Oñate and D.R.J. Owen (Eds)

FINITE POINTSET METHOD (FPM): OPTIMIZED MESHFREE SOLVER FOR AIRBAG DEPLOYMENT SIMULATIONS

JÖRG KUHNERT[*] , LARS ASCHENBRENNER[†] AND ALAIN TRAMEÇON[#]

[*] Fraunhofer Institut für Techno- und Wirtschaftsmathematik (ITWM)
(Fraunhofer Institute for Industrial Mathematics)
Frauhnofer Platz 1, 67663 Kaiserslautern, Germany
e-mail: joerg.kuhnert@itwm.fraunhofer.de, www.itwm.fraunhofer.de

[†] Volkswagen AG
38436 Wolfsburg, Germany
email: lars.aschenbrenner@volkswagen.de, www.volkswagen.de

[#] Engineering Systems International, ESI Group
99 rue des Solets, 94513 Rungis, France
email: atr@esi-group.com, www.esi-group.com

Key words: Meshfree Methods, General Finite Difference Scheme, Airbag Deployment.

Abstract. This document provides an outline of the complete numerical scheme of the Finite Pointset Method (FPM), a meshfree general Finite Difference idea to simulate gasdynamics. The method uses a specialized upwind formulation as well as specialized discrete numerical differential operators in order to gain accuracy as well as stability. The scheme is completed by a k-epsilon turbulence model in order to account for viscous effects. Industrially, FPM performs in airbag deployment modelling as a part of full crash simulations in vehicle design and development.

1 INTRODUCTION

The Finite Pointset Method (FPM) is a generalized numerical tool for simulations in fluid and continuum mechanics. It uses a generalized least squares approach for numerical approximation of derivatives on non-structured point clouds. This procedure turns out to be a generalized finite difference idea with the interesting effect that it reduces to classical finite differences, if the points would be placed in a regular grid.

The character of FPM is Lagrangian, i.e. the particles (points) of the point cloud move with fluid velocity. This turns the method into a very adaptive tool, especially regarding moving parts of the geometry and free surfaces.

In this article, we show how to develop an FPM scheme for compressible fluid flow with viscous effects as well as turbulence modelling. In fact, the differential equations have a strongly hyperbolic character, such that we need to provide a clever upwind scheme (section 2). The numerical integration of turbulences provides the main partition of the system's viscosity and, therefore, requires particular attention (section 3). The special meshfree

(general finite difference) operators used by FPM are explained in section 4. The whole method is industrially applied for airbag deployment simulations in many vehicle manufacturing companies (section 5).

Nomenclature: throughout the paper, a tilde sign (~) in conjunction with differential operators always mean the numerical approximation by the FPM-specialized numerical differential operators.

2 NUMERICAL SCHEME FOR COMPRESSIBLE GASDYNAMICS IN LAGRANGIAN FORM

For modelling gas dynamics flows, we have to consider the laws for conservation of mass, momentum, and energy. Their representation in differential from can be written down in material derivatives (change of the values along a particle path), also known as Lagrangian formulation. FPM will make use of this because it is based on a cloud of numerical points that move with fluid velocity.

2.1 Differential equations to be considered

Let us first have a look at the differential equations of flow motion to be considered here.

General 3D Euler equations (no viscosity)

The general 3D Euler equations for in-viscid gas dynamics on a Lagrangian basis are

$$\begin{aligned} &\tfrac{\mathrm{d}}{\mathrm{dt}}\rho + \rho\cdot\nabla^T\mathbf{v} = 0 \\ &\tfrac{\mathrm{d}}{\mathrm{dt}}(\rho\mathbf{v}) + (\rho\mathbf{v})\cdot\nabla^T\mathbf{v} + \nabla p = 0 \\ &\tfrac{\mathrm{d}}{\mathrm{dt}}(\rho E) + (\rho E)\cdot\nabla^T\mathbf{v} + \nabla^T(p\cdot\mathbf{v}) = 0 \end{aligned} \tag{1}$$

The variables used are

$$\rho = \text{denisty}, \quad \rho\mathbf{v} = \text{momentum}, \quad \rho E = \rho\int c_v dT + \frac{1}{2}\rho\left(\mathbf{v}^T\cdot\mathbf{v}\right)+\rho k = \text{total energy},$$

$$\mathbf{v} = \begin{pmatrix} u & v & w \end{pmatrix}^T = \text{velocity vector}, \quad p = \text{pressure}, \quad k = \text{turbulent kinetic energy}$$

Resulting 1D scheme in primitive form

Let us first assume that there are no turbulent effects, i.e. $k = 0$. Out of (1), the resulting 1D scheme is

$$\begin{aligned} &\tfrac{\mathrm{d}}{\mathrm{dt}}\rho + \rho\cdot\frac{\partial u}{\partial x} = 0 \\ &\tfrac{\mathrm{d}}{\mathrm{dt}}(\rho u) + (\rho u)\cdot\frac{\partial u}{\partial x} + \frac{\partial p}{\partial x} = 0 \\ &\tfrac{\mathrm{d}}{\mathrm{dt}}(\rho E) + (\rho E)\cdot\frac{\partial u}{\partial x} + \frac{\partial(pu)}{\partial x} = 0 \end{aligned} \tag{2}$$

The set of differential equations (2) is in conservative form. For analytical reasons, it will be more useful in the primitive form. Hence, with the help of the thermodynamic identity

$\frac{d}{dt}p = \left.\frac{\partial p}{\partial \rho}\right|_T \cdot \left(\frac{d}{dt}\rho\right) + \left.\frac{\partial p}{\partial T}\right|_\rho \left(\frac{d}{dt}T\right)$ and the definition of the sound speed by $c^2 \equiv \left.\frac{\partial p}{\partial \rho}\right|_T + \frac{p}{c_v \cdot \rho^2}\left.\frac{\partial p}{\partial T}\right|_\rho$, we derive the primitive form of (2) as to be

$$\begin{aligned} \frac{d}{dt}\rho + \rho \cdot \frac{\partial u}{\partial x} &= 0 \\ \frac{d}{dt}u + \frac{1}{\rho}\frac{\partial p}{\partial x} &= 0 \\ \frac{d}{dt}p + \rho c^2 \cdot \frac{\partial u}{\partial x} &= 0 \end{aligned} \tag{3}$$

2.2 Derivation of a scheme 1D scheme by characteristic analysis

The system (3) is perfect for numerical analysis. We would like to establish a stable scheme for this system, well knowing that it is of hyperbolic character. If we are applying a centralized FPM scheme (i.e. using centralized approximations for the occurring derivatives $\frac{\partial u}{\partial x}$ and $\frac{\partial p}{\partial x}$), then we will encounter unstable behaviour of the numerical solution. We suggest therefore a local numerical viscosity in order to stabilize the scheme. First, we need to decouple the system of equations (3) into separate, characteristic differential equations. In compact form, the equations (3) can be written down as

$$\frac{d\mathbf{V}}{dt} + \mathbf{M} \cdot \frac{\partial \mathbf{V}}{\partial x} = \mathbf{0} \tag{4}$$

The matrix $\mathbf{M}$ can be decomposed into its eigenvectors $\mathbf{L} \cdot \mathbf{M} = \mathbf{\Lambda} \cdot \mathbf{L}$, and we explicitly have

$$\mathbf{V} = \begin{pmatrix} \rho \\ u \\ p \end{pmatrix} \quad \mathbf{M} = \begin{pmatrix} 0 & \rho & 0 \\ 0 & 0 & 1/\rho \\ 0 & \rho c^2 & 0 \end{pmatrix} \quad \mathbf{\Lambda} = \begin{pmatrix} 0 & & \\ & c & \\ & & -c \end{pmatrix} \quad \mathbf{L} = \begin{pmatrix} -c^2 & 0 & 1 \\ 0 & \rho c & 1 \\ 0 & -\rho c & 1 \end{pmatrix} \tag{5}$$

Thus, (4) appears as

$$\mathbf{L} \cdot \frac{d\mathbf{V}}{dt} + \mathbf{\Lambda} \cdot \mathbf{L} \frac{\partial \mathbf{V}}{\partial x} = \mathbf{0}, \tag{6}$$

and the resulting scheme in expanded form can be written as

$$\begin{aligned} -c^2 \cdot \frac{d}{dt}\rho + \frac{d}{dt}p &= 0 \\ \frac{d}{dt}(\rho cu + p) + c \cdot \frac{\partial}{\partial x}(\rho cu + p) &= u\left(\frac{d}{dt}(\rho c) + c \cdot \frac{\partial}{\partial x}(\rho c)\right) \\ \frac{d}{dt}(-\rho cu + p) - c \cdot \frac{\partial}{\partial x}(-\rho cu + p) &= -u\left(\frac{d}{dt}(\rho c) - c \cdot \frac{\partial}{\partial x}(\rho c)\right) \end{aligned} \tag{7}$$

The scheme (7) consist of several, uncoupled scalar differential equations, each of which represent a separate transport task of the form

$$\frac{\mathrm{d}}{\mathrm{dt}}\phi \pm \mathrm{c}\cdot\frac{\partial}{\partial \mathrm{x}}\phi = 0 \tag{8}$$

for the dedicated pieces of information $\phi=(\rho \mathrm{cu}+\mathrm{p})$, $\phi=(-\rho \mathrm{cu}+\mathrm{p})$ as well as $\phi=\rho \mathrm{c}$, also referred to as the characteristic items. The term $\pm \mathrm{c}$ is the corresponding, characteristic speed of transport. It is not surprising, that its absolute value for each of the single characteristic items turns out to be the sound speed.

Upwind scheme leading to local viscosity terms

A very simple and stable explicit numerical scheme for (8) is

$$\phi_i^{n+1}=\phi^{n+1}\left(\mathbf{x}_i\right)=\phi^n\left(\mathbf{x}_i \pm c\cdot\Delta t\right), \tag{9}$$

with the time step size Δt. "i" is the particle index and "n", "n+1" represent the discrete time levels. The value of the term $\phi^n\left(\mathbf{x}_i - c\cdot\Delta t\right)$ cannot be provided immediately, either a precise numerical, least squares-like approximation of the quantity ϕ at the location $\left(\mathbf{x}_i \pm c\cdot\Delta t\right)$ can be provided such that the scheme turns out to be $\phi_i^{n+1}=\tilde{\phi}^n\left(\mathbf{x}_i \pm c\cdot\Delta t\right)$, or by a Taylor-series expansion we find $\phi^n\left(\mathbf{x}_i - c\cdot\Delta t\right)=\phi_i^n - c\cdot\Delta t\left.\frac{\partial\phi}{\partial x}\right|_i + \frac{\left(c\cdot\Delta t\right)^2}{2}\left.\frac{\partial^2\phi}{\partial^2 x}\right|_i + HOT$. By using again the least squares approximations for the derivatives and neglecting the higher order terms (HOT), the numerical solution turns out to be

$$\phi_i^{n+1}=\phi_i^n \pm c\cdot\Delta t\left(\left.\frac{\tilde{\partial}\phi}{\tilde{\partial}x}\right|_i \pm \frac{\left(c\cdot\Delta t\right)}{2}\left.\frac{\tilde{\partial}^2\phi}{\tilde{\partial}^2 x}\right|_i\right) \tag{10}$$

In other words, scheme (10) is a first order approximation of a model equation, which enhances (8) by a diffusion term:

$$\frac{\mathrm{d}}{\mathrm{dt}}\phi \pm \mathrm{c}\cdot\frac{\partial}{\partial \mathrm{x}}\phi = \frac{\partial}{\partial \mathrm{x}}\left(\eta\cdot\frac{\partial}{\partial}\phi\right) \tag{11}$$

The right hand side can be considered as the numerical viscosity, the simplest choice is, due to (10), given by $\eta=\frac{c^2\cdot\Delta t}{2}$. However, η accounts also for the higher order terms, and thus, in a more general sense, we establish a local quantification of η by first numerically solving (8) without viscosity and assigning local values of η based on the local overshoots or instabilities. The final numerical solution for one time step is then produced by integration of equation (11).

Stabilized 1D scheme

Numerical stabilization of the scheme (7) naturally follows from (11) by enhancing the transport terms by the numerical viscosity terms:

$$
\begin{aligned}
&-c^2 \cdot \tfrac{d}{dt}\rho + \tfrac{d}{dt}p = 0 \\
&\tfrac{d}{dt}(p+\rho cu)+c\cdot(p+\rho cu)_x = u\left(\tfrac{d}{dt}(\rho c)+c\cdot(\rho c)_x\right) + \left(\eta^+(p+\rho cu)_x\right)_x - u\left(\mu^+(\rho c)_x\right)_x \\
&\tfrac{d}{dt}(p-\rho cu)-c\cdot(p-\rho cu)_x = -u\left(\tfrac{d}{dt}(\rho c)-c\cdot(\rho c)_x\right)+\left(\eta^-(p-\rho cu)_x\right)_x + u\left(\mu^-(\rho c)_x\right)_x
\end{aligned}
\tag{12}
$$

with artificial numerical viscosity terms η^+ , μ^+, η^-, and μ^-, the size of which can be determined by the locally given state. The sub-indices u_x signify, of course, least squares approximation of the derivative with respect to x. Equation (12) can analytically by solved for the time change rates of density, velocity, and pressure, which results in

$$
\begin{aligned}
&\tfrac{d}{dt}\rho + \rho\cdot u_x = \frac{1}{c^2}\left(\eta p_x\right)_x \\
&\tfrac{d}{dt}u + \frac{1}{\rho}p_x = \left(\eta u_x\right)_x \\
&\tfrac{d}{dt}p + \rho c^2\cdot u_x = \left(\eta p_x\right)_x
\end{aligned}
\tag{13}
$$

where we assumed (just for simplicity!) $\eta^+=\mu^+$ and $\eta^-=\mu^-$, and even $\eta=\eta^-+\eta^+$. We suggest a definition of numerical velocity and pressure functions given by

$$
\begin{aligned}
\bar{u} &= u - \eta\cdot\frac{1}{\rho c^2}p_x \\
\bar{p} &= p - \eta\cdot\rho u_x
\end{aligned}
\tag{14}
$$

With this definition and equation (13), we find the modified, but stable, numerical system to be time-integrated

$$
\begin{aligned}
&\tfrac{d}{dt}\rho + \rho\cdot\bar{u}_x = 0 \\
&\tfrac{d}{dt}u + \frac{1}{\rho}\bar{p}_x = 0 \\
&\tfrac{d}{dt}p + \rho c^2\cdot\bar{u}_x = 0
\end{aligned}
\tag{15}
$$

Coming back to the conservative formulation, the above system can be represented as

$$
\begin{aligned}
&\tfrac{d}{dt}\rho = -\rho\cdot\bar{u}_x \\
&\tfrac{d}{dt}(\rho u) = -(\rho u)\cdot\bar{u}_x - \bar{p}_x \\
&\tfrac{d}{dt}(\rho E) = -(\rho E)\cdot\bar{u}_x - (\bar{p}\cdot\bar{u})_x
\end{aligned}
\tag{16}
$$

2.3 Projection of the 1D scheme to the 3D case

In the same fashion as above, we find a system of equations in 3D, which is similar to the equations (16).

$$\begin{aligned}
\tfrac{\mathrm{d}}{\mathrm{dt}}\rho &= -\rho\cdot\tilde{\nabla}^T\overline{\mathbf{v}} \\
\tfrac{\mathrm{d}}{\mathrm{dt}}(\rho\mathbf{v}) &= -(\rho\mathbf{v})\cdot\tilde{\nabla}^T\overline{\mathbf{v}} - \tilde{\nabla}\overline{\mathrm{p}} \\
\tfrac{\mathrm{d}}{\mathrm{dt}}(\rho\mathrm{E}) &= -(\rho\mathrm{E})\cdot\tilde{\nabla}^T\overline{\mathbf{v}} - \tilde{\nabla}^T(\overline{\mathrm{p}}\cdot\overline{\mathbf{v}})
\end{aligned} \tag{17}$$

The symbol $\tilde{\nabla}$ signifies the FPM-specialized moving-least-squares (MLS) gradient operator, see also section 4. Similarly, $\tilde{\Delta}$ for example represents the FPM-MLS approximation of the Laplace operator, which will be used later on. The numerical pressure and velocity expressions are

$$\begin{aligned}
\overline{\mathbf{v}} &= \begin{pmatrix}\overline{\mathrm{u}} & \overline{\mathrm{v}} & \overline{\mathrm{w}}\end{pmatrix}^T \equiv \mathbf{v} - \eta_{\mathrm{p}}\tilde{\nabla}\mathrm{p} \\
\overline{\mathrm{p}} &\equiv \mathrm{p} - \eta_{\mathrm{v}}\tilde{\nabla}^T\mathbf{v}
\end{aligned} \tag{18}$$

By virtue of equation (14) we define

$$\begin{aligned}
\eta_{\mathrm{p}} &= \eta_{\mathrm{num}}\cdot\left(1/\rho c^2\right) \\
\eta_{\mathrm{v}} &= \eta_{\mathrm{num}}\cdot\rho
\end{aligned} \tag{19}$$

We will later see, that η_{num} plays an important role as numerical stabilization quantity. For example, η_v has nearly the same character as a physical viscosity. For the present chapter, let us assume that we know the values of η_{num} at any location

2.4 Adding viscosity to the numerical scheme

In order to treat viscous effects, that come into play for example by the consideration of turbulent motion, scheme (17) has to be enhanced by the viscous stress tensor

$$\begin{aligned}
\tfrac{\mathrm{d}}{\mathrm{dt}}\rho &= -\rho\cdot\tilde{\nabla}^T\overline{\mathbf{v}} \\
\tfrac{\mathrm{d}}{\mathrm{dt}}(\rho\mathbf{v}) &= -(\rho\mathbf{v})\cdot\tilde{\nabla}^T\overline{\mathbf{v}} - \tilde{\nabla}\overline{\mathrm{p}} + \left(\tilde{\nabla}^T\overline{\mathbf{S}}\right)^T \\
\tfrac{\mathrm{d}}{\mathrm{dt}}(\rho\mathrm{E}) &= -(\rho\mathrm{E})\cdot\tilde{\nabla}^T\overline{\mathbf{v}} - \tilde{\nabla}^T(\overline{\mathrm{p}}\cdot\overline{\mathbf{v}}) + \tilde{\nabla}^T(\overline{\mathbf{S}}\cdot\overline{\mathbf{v}})
\end{aligned} \tag{20}$$

The viscous stress tensor in fact is a numerical model of the classical stress tensor of the form

$$\overline{\mathbf{S}} = \overline{\eta}\cdot\left(\tilde{\nabla}\mathbf{v}^T + \left(\tilde{\nabla}\mathbf{v}^T\right)^T - \tfrac{2}{3}\left(\tilde{\nabla}^T\mathbf{v}\right)\cdot\mathbf{I}\right) \tag{21}$$

With the definition of the effective numerical viscosity, given by $\overline{\eta} = \eta_{visc} + \eta_{turb}$. In the same fashion, the laminar viscous and turbulent partitions of the stress tensor can be defined as

$$\begin{aligned}
\mathbf{S}_{turb} &= \eta_{turb}\cdot\left(\tilde{\nabla}\mathbf{v}^T + \left(\tilde{\nabla}\mathbf{v}^T\right)^T - \tfrac{2}{3}\left(\tilde{\nabla}^T\mathbf{v}\right)\cdot\mathbf{I}\right) \\
\mathbf{S}_{visc} &= \eta_{visc}\cdot\left(\tilde{\nabla}\mathbf{v}^T + \left(\tilde{\nabla}\mathbf{v}^T\right)^T - \tfrac{2}{3}\left(\tilde{\nabla}^T\mathbf{v}\right)\cdot\mathbf{I}\right)
\end{aligned} \tag{22}$$

which will be needed later on.

3 NUMERICAL INTEGRATION OF TURBULECE

We will model the k-epsilon turbulence idea within the FPM framework.

3.1 Differential equations of the k-epsilon model

For the purpose of this paper, we will concentrate on the k-epsilon-turbulence formulation. The model equations are

$$\begin{aligned}\frac{d(\rho k)}{dt} &= \nabla^T\left(\left(\eta_{visc}+\frac{\eta_{turb}}{\sigma_k}\right)\nabla k\right) - \rho\varepsilon + P_k + P_b \\ \frac{d(\rho\varepsilon)}{dt} &= \nabla^T\left(\left(\eta_{visc}+\frac{\eta_{turb}}{\sigma_\varepsilon}\right)\nabla\varepsilon\right) - C_{2\varepsilon}\rho\frac{\varepsilon^2}{k} + C_{1\varepsilon}\frac{\varepsilon}{k}\cdot\left(P_k + P_b\right)\end{aligned} \tag{23}$$

Here, P_k means the turbulent production rate, and it is determined by

$$P_k = \nabla^T\left(\mathbf{S}_{turb}\cdot\mathbf{v}\right) - \left(\nabla^T\mathbf{S}_{turb}\right)\cdot\mathbf{v} = \eta_{turb}\cdot\|\mathbf{D}\|_M^2 \tag{24}$$

A similar expression, P_b, is dedicated to turbulent buoyancy effects, which will be neglected for this paper. The turbulent viscosity is a function of the turbulent quantities k and epsilon, represented by $\eta_{turb} = \rho\cdot C_\eta\cdot\frac{k^2}{\varepsilon}$. The given model constants are σ_k, σ_ε, $C_{2\varepsilon}$, $C_{1\varepsilon}$, C_η, and finally,

$$\|\mathbf{D}\|_M^2 = \left(v_x+u_y\right)^2 + \left(w_x+u_z\right)^2 + \left(v_z+w_y\right)^2 + \tfrac{2}{3}\left(u_x-v_y\right)^2 + \tfrac{2}{3}\left(v_y-w_z\right)^2 + \tfrac{2}{3}\left(w_z-u_x\right)^2$$

provides, in fact, the Mises-norm of the symmetric part of the velocity gradient, which ensures that the turbulent production rate be always positive.

3.2 Numerical evolution scheme and time integration of the k-epsilon model

The numerical evolution scheme

$$\begin{aligned}\frac{d(\rho k)}{dt} &= \tilde{\nabla}^T\left(\left(\eta+\frac{\eta_{turb}}{\sigma_k}\right)\tilde{\nabla}k\right) - \rho\varepsilon + P_k \\ \frac{d(\rho\varepsilon)}{dt} &= \tilde{\nabla}^T\left(\left(\eta+\frac{\eta_{turb}}{\sigma_\varepsilon}\right)\tilde{\nabla}\varepsilon\right) - C_{2\varepsilon}\rho\frac{\varepsilon^2}{k} + C_{1\varepsilon}\frac{\varepsilon}{k}\cdot P_k\end{aligned}, \tag{25}$$

just arises by replacing the spatial derivatives in (23) by its FPM-MLS operators. For better numerical analysis, we can rewrite this scheme by replacing P_k by its formal expression (24)

$$\begin{aligned}\frac{d(k)}{dt} &= \frac{1}{\rho}\left(\tilde{\Delta}_{\eta}k\right) - \varepsilon + C_\eta\frac{k^2}{\varepsilon}\|\mathbf{D}\|_M^2 \\ \frac{d(\varepsilon)}{dt} &= \frac{1}{\rho}\left(\tilde{\Delta}_{\eta}\varepsilon\right) - C_{2\varepsilon}\frac{\varepsilon^2}{k} + C_{1\varepsilon}C_\eta\cdot k\cdot\|\mathbf{D}\|_M^2\end{aligned} \tag{26}$$

From system (26), we derive a singularity formulation, which is either

$$\frac{\mathrm{d}}{\mathrm{dt}}\left(\frac{\mathrm{k}}{\varepsilon}\right) \;=\; \left(\mathrm{C}_{2\varepsilon}-1\right) \;+\; \mathrm{C}_{\eta}\left(1-\mathrm{C}_{1\varepsilon}\right)\left\|\mathbf{D}\right\|_{M}^{2}\cdot\left(\frac{\mathrm{k}}{\varepsilon}\right)^{2} \;+\; \frac{1}{\rho}\left(\tilde{\Delta}_{\hat{\eta}}\,\frac{\mathrm{k}}{\varepsilon}\right) \tag{27}$$

or

$$\frac{\mathrm{d}}{\mathrm{dt}}\left(\frac{\varepsilon}{\mathrm{k}}\right) \;=\; \left(1-\mathrm{C}_{2\varepsilon}\right)\cdot\left(\frac{\varepsilon}{\mathrm{k}}\right)^{2} \;+\; \mathrm{C}_{\eta}\left(\mathrm{C}_{1\varepsilon}-1\right)\left\|\mathbf{D}\right\|_{M}^{2} \;+\; \frac{1}{\rho}\left(\tilde{\Delta}_{\hat{\eta}}\left(\frac{\varepsilon}{\mathrm{k}}\right)\right) \tag{28}$$

If not both values k and ε are zero, we can provide numerical mean values

$$\left.\frac{\mathrm{k}}{\varepsilon}\right|_{mean} = \frac{1}{\Delta\mathrm{t}}\int_{0}^{\Delta\mathrm{t}}\left(\frac{\mathrm{k}}{\varepsilon}\right)dt \quad \text{and} \quad \left.\frac{\varepsilon}{\mathrm{k}}\right|_{mean} = \frac{1}{\Delta\mathrm{t}}\int_{0}^{\Delta\mathrm{t}}\left(\frac{\varepsilon}{\mathrm{k}}\right)dt\,. \tag{29}$$

It remains to state a possibly precise numerical time integration method of the scheme (26) where we avoid singularities by using the mean values (29). Thus, the numerical evolution scheme can be written as

$$\begin{aligned}
\frac{\mathrm{d}(\mathrm{k})}{\mathrm{dt}} &= \frac{1}{\rho}\left(\tilde{\Delta}_{\hat{\eta}}\mathrm{k}\right) - \left(\left.\frac{\varepsilon}{\mathrm{k}}\right|_{mean}\right)\cdot\mathrm{k} + \mathrm{C}_{\eta}\cdot\left(\left.\frac{\mathrm{k}}{\varepsilon}\right|_{mean}\right)\mathrm{k}\left\|\mathbf{D}\right\|_{M}^{2} \\
\frac{\mathrm{d}(\varepsilon)}{\mathrm{dt}} &= \frac{1}{\rho}\left(\tilde{\Delta}_{\hat{\eta}}\varepsilon\right) - \mathrm{C}_{2\varepsilon}\cdot\left(\left.\frac{\varepsilon}{\mathrm{k}}\right|_{mean}\right)\cdot\varepsilon + \mathrm{C}_{1\varepsilon}\mathrm{C}_{\eta}\cdot\left(\left.\frac{\mathrm{k}}{\varepsilon}\right|_{mean}\right)\cdot\varepsilon\cdot\left\|\mathbf{D}\right\|_{M}^{2}
\end{aligned} \tag{30}$$

for which we can now apply a numerical integration that guaranties the positivity of the terms k and ε. It is based on semi-implicit first order time stepping, given by

$$\begin{aligned}
\frac{\mathrm{k}^{n+1}-\mathrm{k}^{n}}{\Delta\mathrm{t}} &= \frac{1}{\rho}\left(\tilde{\Delta}_{\hat{\eta}}\mathrm{k}^{n}\right) - \left(\left.\frac{\varepsilon}{\mathrm{k}}\right|_{mean}\right)\cdot\mathrm{k}^{n+1} + \mathrm{C}_{\eta}\cdot\left(\left.\frac{\mathrm{k}}{\varepsilon}\right|_{mean}\right)\left\|\mathbf{D}\right\|_{M}^{2}\cdot\mathrm{k}^{n} \\
\frac{\varepsilon^{n+1}-\varepsilon^{n}}{\Delta\mathrm{t}} &= \frac{1}{\rho}\left(\tilde{\Delta}_{\hat{\eta}}\varepsilon^{n}\right) - \mathrm{C}_{2\varepsilon}\cdot\left(\left.\frac{\varepsilon}{\mathrm{k}}\right|_{mean}\right)\cdot\varepsilon^{n+1} + \mathrm{C}_{1\varepsilon}\mathrm{C}_{\eta}\cdot\left(\left.\frac{\mathrm{k}}{\varepsilon}\right|_{mean}\right)\cdot\left\|\mathbf{D}\right\|_{M}^{2}\cdot\varepsilon^{n}
\end{aligned} \tag{31}$$

3.3 Analytical evaluation of the mean values of the singular terms

The singular terms $\left.\frac{\mathrm{k}}{\varepsilon}\right|_{mean} = \frac{1}{\Delta\mathrm{t}}\int_{0}^{\Delta\mathrm{t}}\left(\frac{\mathrm{k}}{\varepsilon}\right)dt$ and $\left.\frac{\varepsilon}{\mathrm{k}}\right|_{mean} = \frac{1}{\Delta\mathrm{t}}\int_{0}^{\Delta\mathrm{t}}\left(\frac{\varepsilon}{\mathrm{k}}\right)dt$ need to be evaluated analytically in order to provide acceptable values for integration scheme (31). If we assume negligibility of the diffusion term $\frac{1}{\rho}\left(\tilde{\Delta}_{\hat{\eta}}\left(\frac{\varepsilon}{\mathrm{k}}\right)\right)$ in equation (27), it reduces to $\frac{\mathrm{d}}{\mathrm{dt}}\left(\frac{\mathrm{k}}{\varepsilon}\right) \;=\; \left(\mathrm{C}_{2\varepsilon}-1\right) \;+\; \mathrm{C}_{\eta}\left(1-\mathrm{C}_{1\varepsilon}\right)\left\|\mathbf{D}\right\|_{M}^{2}\cdot\left(\frac{\mathrm{k}}{\varepsilon}\right)^{2}$, and more simple

$$\frac{\mathrm{d}}{\mathrm{dt}}\mathrm{x} \;=\; A \;-\; B\cdot\mathrm{x}^{2} \tag{32}$$

Here, $\mathrm{x} = \frac{\varepsilon}{\mathrm{k}}$, $A = \left(\mathrm{C}_{2\varepsilon} - 1\right)$, and $B = \mathrm{C}_{\eta}\left(\mathrm{C}_{1\varepsilon} - 1\right)\left\|\mathbf{D}\right\|_M^2$. The analytical solution to (32) is

$$x = \sqrt{A/B}\tanh\left(\sqrt{AB}\left(t - t_0\right) + arc\tanh\left(\sqrt{B/A}x_0\right)\right) \tag{33}$$

as well as

$$x = \sqrt{A/B}\coth\left(\sqrt{AB}\left(t - t_0\right) + arc\coth\left(\sqrt{B/A}x_0\right)\right) \tag{34}$$

The arctanh is defined between -1 and 1, the arccoth complementary. Hence, the choice of the solution (33) or (34) depends on $x_0 > \sqrt{A/B}$ or $x_0 < \sqrt{A/B}$.

3.4 Boundary conditions for solid walls

The solid wall particles in FPM can be treated like interior particles, with one exception: the wall particles are assumed to be shifted to the interior of the flow domain by a small value $\alpha \cdot h$. Thus, in the model (30) , the term $\frac{1}{\rho}\left(\tilde{\Delta}_{\hat{\eta}}\mathrm{k}\right)$ need to have an additional contribution, i.e. the contribution that comes from the fact that the velocity drops to zero exactly at the wall. In this sense, we obtain the enhanced model by

$$\frac{\mathrm{d}\left(\mathrm{k}\right)}{\mathrm{dt}} = \frac{1}{\rho}\left(\tilde{\Delta}_{\hat{\eta}}\mathrm{k}\right) - \left(\frac{\varepsilon}{\mathrm{k}}\bigg|_{mean}\right)\cdot\mathrm{k} + \mathrm{C}_{\eta}\cdot\left(\frac{\mathrm{k}}{\varepsilon}\bigg|_{mean}\right)\mathrm{k}\left\|\mathbf{D}\right\|_M^2 + \frac{\hat{\eta}}{\rho}\cdot\left(\frac{\partial\mathrm{k}}{\partial\mathrm{n}} - \frac{\mathrm{k}}{\alpha\cdot h}\right)\cdot\frac{1}{\frac{1}{2}\left(\alpha\cdot h + \frac{1}{2}h\right)}$$

$$\frac{\mathrm{d}\left(\varepsilon\right)}{\mathrm{dt}} = \frac{1}{\rho}\left(\tilde{\Delta}_{\hat{\eta}}\varepsilon\right) - \mathrm{C}_{2\varepsilon}\cdot\left(\frac{\varepsilon}{\mathrm{k}}\bigg|_{mean}\right)\cdot\varepsilon + \mathrm{C}_{1\varepsilon}\mathrm{C}_{\eta}\cdot\left(\frac{\mathrm{k}}{\varepsilon}\bigg|_{mean}\right)\cdot\varepsilon\cdot\left\|\mathbf{D}\right\|_M^2 + \frac{\hat{\eta}}{\rho}\cdot\left(\frac{\partial\varepsilon}{\partial\mathrm{n}} - \frac{\varepsilon}{\alpha\cdot h}\right)\cdot\frac{1}{\frac{1}{2}\left(\alpha\cdot h + \frac{1}{2}h\right)}$$

4 MEHSFREE DIFFERENTIAL OPERATORS

4.1 Definition of Differential operators

Let us suppose there is a pointcloud being sufficiently dense. The positions of the particles are given by $\mathbf{x}_i = \left(x_i \;\; y_i \;\; z_i\right)^T$, $i = 1...N$, and N is the number of particles. Suppose furthermore that some function f is given only at the discrete particle locations, i.e. $f_i \equiv f\left(\mathbf{x}_i\right)$. The vector of discrete function values is given by $\mathbf{f} \equiv \left(f_1, f_2, ..., f_N\right)^T$. We call the numerical differential operators in FPM those vectors which provide an approximation of some derivative in the sense

$$\partial^*_{numerical} f\left(\mathbf{x}_i\right) = \tilde{\partial}^* f\left(\mathbf{x}_i\right) = \tilde{\partial}^* f_i = \sum_{j=1}^{N} c^*_{ij}\cdot f_j = \left(\mathbf{c}^*_i\right)^T\cdot\mathbf{f} \tag{35}$$

The star (*) in the equation above is a placeholder for all the numerous differential operators needed by FPM. In that aspect, $\mathbf{c}_i^0$ would be the numerical operator for function approximation, $\mathbf{c}_i^x$, $\mathbf{c}_i^y$, $\mathbf{c}_i^z$ the respective operators for the x, y, and z derivatives, and $\mathbf{c}_i^{\Delta}$ the one for approximation of the Laplacien. Just to name the most often appearing ones. Our goal

is to develop operators which are, as shown in (35), independent on the underlying function values. Having operators which work generally for all given functions will save a lot of computation time. We also introduce a weight function which switches on the particular neighbours close to some particle i.

$$W_{ij} = w\left(r\left(\mathbf{x}_i, \mathbf{x}_j\right)\right) = w\left(r_{ij}\right), \qquad r\left(\mathbf{x}_i, \mathbf{x}_j\right) = \left\|\mathbf{x}_i - \mathbf{x}_j\right\| \Big/ \tfrac{1}{2}\left(h\left(\mathbf{x}_i\right) + h\left(\mathbf{x}_j\right)\right) \tag{36}$$

The function $h\left(\mathbf{x}_i\right)$ is referred to as smoothing length, turning out to be the maximum interaction radius between two particles. It actually rules the local density of the particles, i.e. the mean distance between particles. We try to provide a weight function which becomes zero if $r = 1$ and one if $r = 0$ and which is n-times continuously differentiable. For example

$$w(r) = \begin{cases} \left(1 - r^2\right)^{\gamma}, & \text{if } r < 1 \\ 0, & \text{otherwise} \end{cases} \tag{37}$$

We can write the discrete weight values on the diagonal of the so called weight matrix

$$\mathbf{W}_i = \begin{pmatrix} w_{i1} & & & 0 \\ & w_{i2} & & \\ & & \ddots & \\ 0 & & & w_{iN} \end{pmatrix} \tag{38}$$

having the discrete weights on its diagonal and zeros otherwise.

4.2 General least squares procedure for operators

We are searching for the operator $\mathbf{c}_i$ fulfilling the least squares criterion

$$\frac{1}{2}\left\|\mathbf{W}_i^{-1} \cdot \mathbf{c}_i\right\|^2 = \frac{1}{2}\mathbf{c}_i^T \cdot \mathbf{W}_i^{-1T} \cdot \mathbf{W}_i^{-1} \cdot \mathbf{c}_i = \frac{1}{2}\mathbf{c}_i^T \cdot \mathbf{W}_i^{-2} \cdot \mathbf{c}_i \overset{!}{=} \min \tag{39}$$

under the consistency conditions

$$\mathbf{K}_i^T \cdot \mathbf{c}_i = \mathbf{b} \tag{40}$$

The matrix $\mathbf{K}_i$ represents test functions (given as discrete values at the particles) for which the numerical operator are forced to give a distinct value. As for example, the numerical operator for the x-derivative $\mathbf{c}_i^x$ shall deliver zero if operating on a constant function $\mathbf{k}_i^0 = (1,\ 1, ..., 1)$ or a quadratic function $\mathbf{k}_i^2 = \left(\left(x_1 - x_i\right)^2,\ \left(x_2 - x_i\right)^2, ..., \left(x_N - x_i\right)^2\right)$, but it shall deliver one if operating on the linear function $\mathbf{k}_i^1 = \left(x_1 - x_i,\ x_2 - x_i, ..., x_N - x_i\right)$. In other words, we have the conditions (among others!)

$$\left(\mathbf{k}_i^0\right)^T \cdot \mathbf{c}_i^x = 0\ , \quad \left(\mathbf{k}_i^1\right)^T \cdot \mathbf{c}_i^x = 1\ , \quad \left(\mathbf{k}_i^2\right)^T \cdot \mathbf{c}_i^x = 0 \tag{41}$$

In general, the matrix $\mathbf{K}$ contains M discretely given test functions, which do not only contain the geometric monomials, but can be enhanced by stability conditions as well. The right hand side vector $\mathbf{b}$ consequently contains the corresponding values to be delivered by

the operator if applied to the test functions. The minimization problem (39) together with the constraints (40) can be solved using Lagrange multipliers.

5 APPLICATIONS TO AIRBAG DEPLOYMENT

5.1 Coupling of FPM into PAM-Crash Software

FPM is linked into the crash analysis software PAM-Crash, provided by ESI Group, France. Here, FPM takes over the simulation of the gasdynamics inside of airbags, a main constructive feature in car design in order to protect drivers and passengers in case of a crash accident.

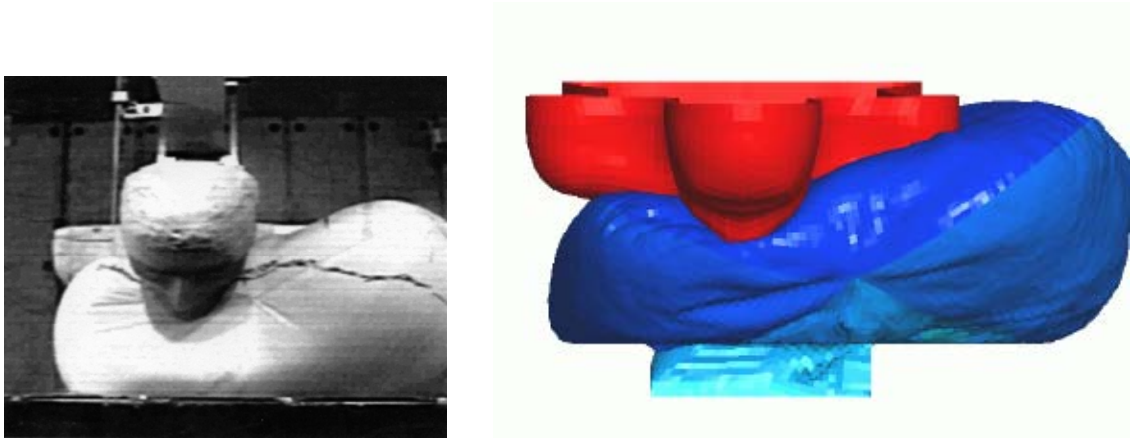

Passengers airbag in experiment and simulation

The coupling between the two codes is strong. In each simulation time step, there is a synchronization and information exchange. During one time step, FPM produces a pressure solution of the gas along the airbag's fabrics, which is communicated to the PAM-Crash software. With this new pressure values, PAM-Crash is able to complete one time step and provide to FPM updated values of the membrane dynamics, such as position as well as velocities of the membrane's node points. This cycle now is repeated during the whole simulation, which means that also the time step sizes of both codes have to be synchronized.

FPM particles showing the velocity vectors in a typical airbag simulation application

5.2 Experimental results vs. numerical simulation

The coupled method is very well validated by experiments. One typical setup is the testing of flat bags, because here any unknown factors of the folding and wrapping of airbag are excluded. In the experiment, the deploying airbag pushes away a pendulum of a certain length and mass. Experimentally, the acceleration of the pendulum is measured and later on compared to the numerical results.

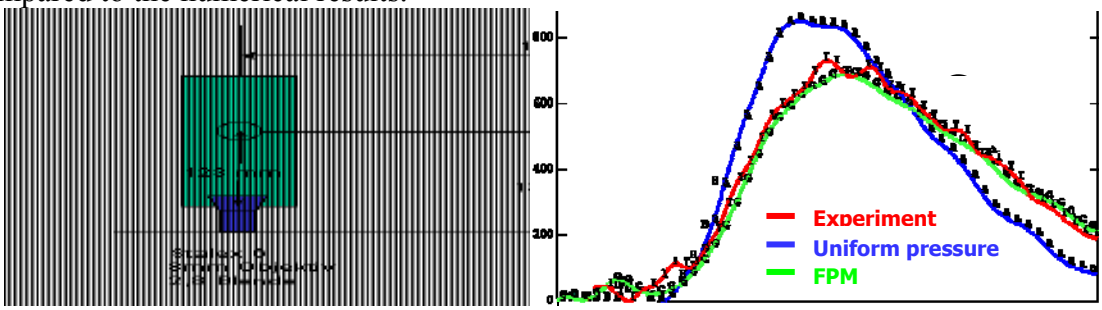

Experimental setup and comparison of the acceleration curve of the pendulum of experiment, uniform pressure method and FPM

5.3 Calibration of the turbulence model

The turbulence model, especially the factor α of section 3.4, is calibrated by experiments. They are conducted in order to correlate the pressure drop, i.e. viscous turbulent force load, inside of a tube with the according mass flux. The measurements contain the pressure difference of the beginning and end of the tube as well as localized measurements of the wall stresses. Both items can be used in order to calibrate the turbulence model, such that it at least provides the same results for these simple applications. Of course, for the experiments, the wall material of the tube is covered with airbag fabrics, such that the correct roughness of the boundaries is set into place.

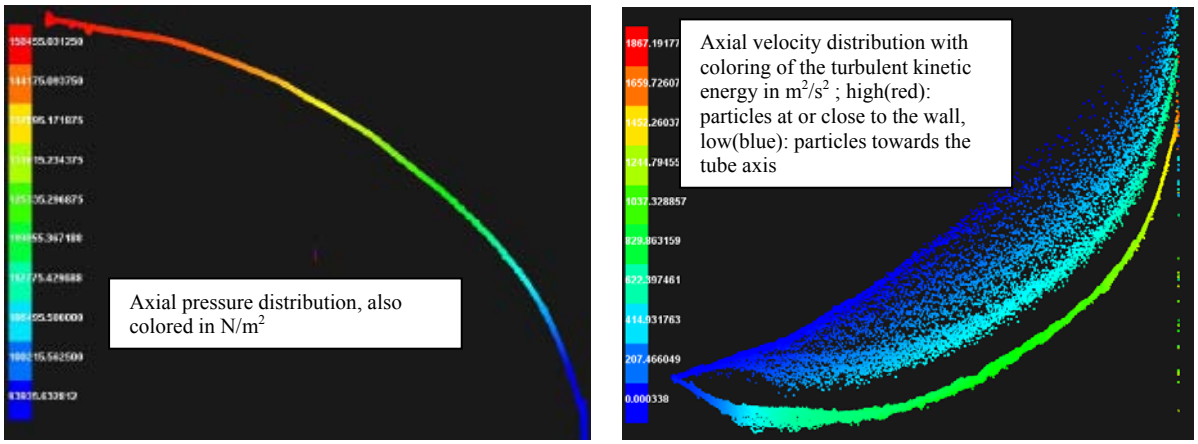

FPM-computed pressure and velocity distributions in the experimental tube setup